Imidazole/(HPO$_3$)$_3$-doped sulfonated poly (ether ether ketone) composite membrane for fuel cells

Shaoying Liu,[1] Yingying Liu,[1] Shangbin Sang,[1] Wenjie Zhong,[1] Qiumei Wu[2]

[1]College of Chemistry and Chemical Engineering, Central South University, Changsha City, Hunan Province, People's Republic of China
[2]Key State Laboratory of Power Metallurgy, Powder Metallurgy Research Institute, Central South University, Changsha City, Hunan Province, Changsha 410083, People's Republic of China
Correspondence to: S. Sang (E-mail: sangsb@126.com) and Q. Wu (E-mail: wuqiumei20073@126.com)

ABSTRACT: A novel gel of imidazole/(HPO$_3$)$_3$ was synthesized and incorporated into sulfonated poly (ether ether ketone) (SPEEK) to fabricate composite proton exchange membranes. The composite membranes were characterized by alternating current impedance (AC), thermogravimetry (TG), differential scanning calorimetry (DSC), X-ray diffraction (XRD), scanning electron microscope (SEM) and mechanical property test. Based on the electrochemical performance investigation, the proton conductivity of the membrane is intimately correlated with the temperature and the mass ratio of imidazole/(HPO$_3$)$_3$ in the composite. The SPEEK/imidazole/(HPO$_3$)$_3$−4 composite membrane (with 44.4 wt % of imidazole/(HPO$_3$)$_3$) has the optimized performance at 135°C. Mover, the strength of the composite membranes is almost comparable to that of Nafion membrane. © 2015 Wiley Periodicals, Inc. J. Appl. Polym. Sci. **2015**, *132*, 41946.

INTRODUCTION

The polymer electrolyte membrane fuel cells (PEMFCs), which are operated at the temperature of 100∼200°C, have attracted much attention as a source of clean energy in the near future, due to their unique advantages, such as higher tolerance to traces of CO, faster electrode kinetics, no cathode flooding and simpler system design.[1,2] Currently, Nafion® (DuPont) is considered to be the most successful membrane because of its high proton conductivity and high chemical stability. However, its proton conductivity is closely related to high levels of hydration, and are insufficient above 100°C due to the loss of water.

Recently, SPEEK shows great potential for PEMs, owing to its good mechanical properties, high chemical resistance, thermal stability and low price in contrast to Nafion®.[3–7] However, the SPEEK with a low degree of sulfonation (DS) generates inferior conductivity, which is detrimental to its practical use in the PEMFC system at intermediate temperatures.

To improve the proton conductivity of anhydrous proton membrane, some liquid solution (e.g., phosphoric acid,[8,9] sulfuric acid[9] and ionic liquid[10,11]) have been introduced into the membrane to enhance proton-transfer ability. Among these additives,

H$_3$PO$_4$ is widely employed as anhydrous proton conductor because of its high proton conductivity, low cost, and thermal stability.[12]

It is well known that the proton conductivity of PEMs depends heavily upon the ionization constant, that is, the pKa of the additives. The pKa of H$_3$PO$_4$ is 2.148[13] under standard conditions. By contrast, the pKa of (HPO$_3$)$_3$ (pKa$_1$ = ∼1)[13] is lower than that of H$_3$PO$_4$, and its conductivity is probably higher than that of H$_3$PO$_4$. Thus it can be expected that polymer/(HPO$_3$)$_3$ composite membranes will have higher proton conductivity. Furthermore, the higher viscosity of (HPO$_3$)$_3$ may make it more suitable to be fixed into the polymer matrix.

On the other hand, heterocyclic molecules (e.g., imidazoles, benzimidazoles, pyrazoles, etc.) are known to allow the protons to transfer even in the non-aqueous condition.[14,15] A higher proton conductivity of 10^{-3} S/cm was reached at the melting point of 90°C[16] for imidazole through hydrogen-bonded ionic channels (Imi$\cdots$ImiH$^+\cdots$Imi route).

In view of the two aspects, it can be expected that polymer/(HPO$_3$)$_3$ composite membranes doped by imidazole may enhance the composite membrane proton conductivity by the

Additional Supporting Information may be found in the online version of this article.

Table I. The Contents of the Composite Membranes

Sample	The mass of SPEEK/g	The mass of the additive/g	The additive ratio in the sample (%)
Pure SPEEk	0.5	0	0
SPEEK/imidazole/(HPO$_3$)$_3$−1	0.5	0.1	16.7
SPEEK/imidazole/(HPO$_3$)$_3$−2	0.5	0.2	28.6
SPEEK/imidazole/(HPO$_3$)$_3$−3	0.5	0.3	37.5
SPEEK/imidazole/(HPO$_3$)$_3$−4	0.5	0.4	44.4
SPEEK/imidazole/(HPO$_3$)$_3$−5	0.5	0.5	50

formation of a proton-transfer channel among polymer matrix, imidazole and (HPO$_3$)$_3$.

In this study, a gel of imidazole/(HPO$_3$)$_3$ was synthesized and doped into SPEEK to fabricate hybrid proton conducting membranes for potential application in PEMFCs. Here, by simply blending imidazole/(HPO$_3$)$_3$ and SPEEK, we investigated systematically the role of imidazole/(HPO$_3$)$_3$ in improving proton conductivity under anhydrous conditions as well as other consequent changes such as thermal stability, mechanical property and morphology.
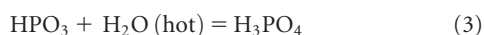
EXPERIMENTAL

Materials and Chemicals

Poly (ether ether ketone) (PEEK 450pf) was purchased from Victrex High-performance Materials Co. All the rest chemical reagents used were Analytical grade, and purchased from Sinopharm Chemical Reagent Co.

Preparation

Preparation of Imidazole/(HPO$_3$)$_3$. The most convenient and inexpensive method for preparing (HPO$_3$)$_3$ is by reacting phosphorus pentoxide (P$_2$O$_5$) with phosphoric acid (H$_3$PO$_4$). The equations are shown below:

$$P_2O_5 + H_2O \text{ (cold)} = 2HPO_3 \tag{1}$$

$$P_2O_5 + 3H_2O \text{ (hot)} = 2H_3PO_4 \tag{2}$$

$$HPO_3 + H_2O \text{ (hot)} = H_3PO_4 \tag{3}$$

$$3H_3PO_4 = (HPO_3)_3 + 3H_2O \tag{4}$$

20.4 g of P$_2$O$_5$ and 5 mL 85 wt % H$_3$PO$_4$ were stirred continuously at 180°C under Ar atmosphere until a yellow semitransparent gel was formed. Keep it under 180°C for 4 h. When the temperature of the gel dropped to 80°C, 3 g of imidazole were added. Then the mixture was stirred continuously at 80°C under Ar atmosphere until a semitransparent gel was formed.

Sulfonation of PEEK. SPEEK was synthesized according to the technique given elsewhere.[6,17,18] PEEK powder was firstly dried in oven at 80°C for 24 h before sulfonation. Then, 7 g of dried PEEK was dissolved into 100 mL concentrated sulfuric acid (H$_2$SO$_4$, 98 wt %) under vigorous stirring at 50°C for 5 h. The obtained solution was added into a large excess of ice-cold water under continuous stirring. Then the white precipitate was removed and washed with deionized water until pH 6 to remove residual acid. Finally, The sulfonated polymer was dried in vacuum oven at 60°C for 24 h.

Preparation of Composite Membranes. SPEEK/imidazole/(HPO$_3$)$_3$ composite membranes were prepared by solution casting method. Dimethylsulfoxide (DMSO) solvent was heated to 80°C in thermostatic magnetic stirring oil bath. Then SPEEK and the gel of imidazole/(HPO$_3$)$_3$ with different proportions were added into DMSO solvent under magnetic stirring. The mixture was stirred in 80°C for 3 h, followed by ultrasonically treatment for 30 min. The mixture was poured out in a mold and dried in vacuum oven at 50°C for 24 h and then at 80°C for 24 h to form a homogeneous membrane. Contents of each component of composite membranes were shown in Table I.

Characterization

Fourier transform infrared (FTIR) spectra were obtained from a Nicolet6700 (Thermo Nicolet Corporation, USA). The spectra were measured in transmittance mode over a wavenumbers range of 4000∼500 cm^{-1}. Proton nuclear magnetic resonance (^{1}H-NMR) spectra were recorded using an AVANCE III 400 (Bruker, Switzerland). The surface morphology of the membranes were observed by Scanning Electron Microscopy (SEM) (Quanta 200 FEG, FEI Company, USA) equipped with an energy dispersive X-ray (EDX) spectrometer. Thermogravimetric (TG) analysis and Differential scanning calorimetry (DSC) of the membranes were performed with SAT449C (Netzsch, Germany) under Ar atmosphere and at a heating rate of 10K min^{-1}. X-ray diffraction measurements (XRD) were performed by X-ray Diffractometer (D/MAX2500, Rigaku, Japan). The mechanical properties of the membranes were determined with a biomechanical testing machine (MTS Insight, USA). The measurements were taken at 20°C and relative humidity of around 50% with the crosshead speed of 10 mm min^{-1}. Proton conductivity was evaluated based on impedance spectroscopy using a PARSTAT2273 (Princeton Applied Research, AMETEK, USA) without extra humidification. Membranes were sandwiched between two stainless-steel electrodes with 1 cm in diameter. Conductivities of membranes were carried out as a function of temperature (from 55°C to 135°C) without extra humidification. Additionally, the thickness of the membranes was measured after the impedance measurements. The membrane conductivity is calculated by:

$$\sigma = L/(R \times S) \tag{5}$$

where σ is proton membrane conductivity, S/cm; L is the thickness of membranes, cm; R is the resistance of membranes, Ω; S is the area of membranes, 0.785 cm^2.
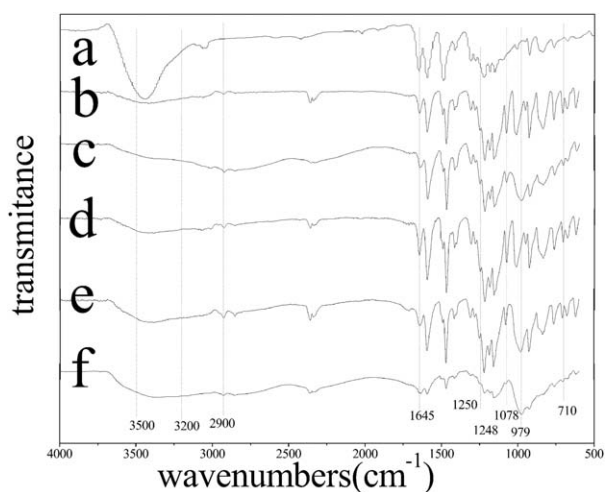
Figure 1. FTIR spectra of PEEK powder (a), pure SPEEK membrane (b), SPEEK/$(HPO_3)_3$ composite membrane (c), SPEEK/imidazole composite membrane (d), SPEEK/imidazole/$(HPO_3)_3$−3 composite membrane (e) and SPEEK/imidazole/$(HPO_3)_3$−4 composite membrane (f).

RESULTS AND DISCUSSION

FTIR Spectra

Figure 1 shows the typical FTIR spectra of PEEK powder, pure SPEEK membrane, SPEEK/$(HPO_3)_3$ composite membrane, SPEEK/imidazole composite membrane (at the same doping content with SPEEK/imidazole/$(HPO_3)_3$−3 composite membrane), SPEEK/imidazole/$(HPO_3)_3$−3 composite membrane and SPEEK/imidazole/$(HPO_3)_3$−4 composite membrane.

In all spectra, aromatic groups from PEEK backbone are observed at 1019 cm^{-1} for —Ar—O—Ar— and 1650 cm^{-1} for —Ar—C(=O)—Ar—. However, the pure SPEEK membrane and composite membranes showed the additional characteristic peaks at 1078 cm^{-1}, 1250 cm^{-1} and 710 cm^{-1} after sulfonation, which are attributed to two O=S=O stretching bands and S—O stretching bands, respectively.

The spectrum of SPEEK/$(HPO_3)_3$ membrane [Figure 1(c)] and SPEEK/imidazole/$(HPO_3)_3$ composite membranes [Figure 1(e,f)] show strong bands at 3500∼3000 cm^{-1} which indicates that $(HPO_3)_3$ interacts with SPEEK mainly by OH···O=S hydrogen bonds.[19] The absorption peak at 979 cm^{-1} is typically attributed to P—O vibration. These results showed that $(HPO_3)_3$ was successfully added into the SPEEK matrix.

The spectrum of SPEEK/imidazole membrane [Figure 1(d)] and SPEEK/imidazole/$(HPO_3)_3$ composite membranes [Figure 1(e,f)] show a broad band at 3500∼3000 cm^{-1} which is attributed to the -OH stretching of the same group and the —N—H stretching.[20,21] Additionally, the stronger absorption band at 1645 cm^{-1} associated with heteroaromatic ring[21,22] and —Ar—C(=O)—Ar—. Hydrogen bond seems to play an important role in the proton conductivity of this system. These results showed that imidazole was successfully added into the SPEEK matrix.

¹H-NMR

The DS was determined through proton nuclear magnetism resonance method. Figure 2 shows the proton nuclear magnetism

resonance of SPEEK. The proton designation of each position was calculated based on Figure 2. The chemical shifts of the designation proton were shown in Table II. The DS was determined according to eqs. (6), (7) [23] which was calculated to be 70.8%.

$$\frac{n}{12-2n} = \frac{S_{H_7}}{\sum_{i=1}^{6} S_{H_i}} \tag{6}$$

$$DS = n \times 100\% \tag{7}$$

where n is the number of —SO$_3$H; S is the peak area of the designation proton.

Morphology of the Composite Membranes

Figure 3 shows the SEM images of the surface of composite membrane at various imidazole/$(HPO_3)_3$ loading. Both S and P element contents are observed by EDX of pure SPEEK membrane and SPEEK/imidazole/$(HPO_3)_3$-2 composite membrane in Figures 4 and 5, respectively. The impregnation of high loading of imidazole/$(HPO_3)_3$ into the polymer matrix has a significant impact on the polymer structure. Excessive loading of imidazole/$(HPO_3)_3$ can cause phase separation and crazing on the surface of composite membranes.

As shown in Figure 3(a,b), the surface of the pure SPEEK membrane and composite membranes at low imidazole/$(HPO_3)_3$ loading ($\leq$16.7 wt %) were very compact and homogeneous without visible micro-pores and phase separation. The conclusion can be supported from EDX spectra of pure SPEEK membrane in Figure 4. Elemental sulfur was homogeneous on the surface of the pure SPEEK membrane.

Figure 3(c) indicates the presence of crazing on the surface of composite membranes when 28.6 wt % imidazole/$(HPO_3)_3$ were embedded. The different phenomenon can be supported from EDX spectra of SPEEK/imidazole/$(HPO_3)_3$−2 composite membrane in Figure 5. The content of S is higher than that of P in the crazing on the surface, and it is contrary to that of other places. So it can be concluded that the hydrophilic group (e.g., imidazole, $(HPO_3)_3$, —SO$_3$H) can be gathered into cluster, and the hydrophobic groups of framework of SPEEK will be coacted outside of the hydrophilic group. Therefore, it will form the crazing between the hydrophobic groups. With the increase of imidazole/$(HPO_3)_3$ content the crazing will be filled with the gel.
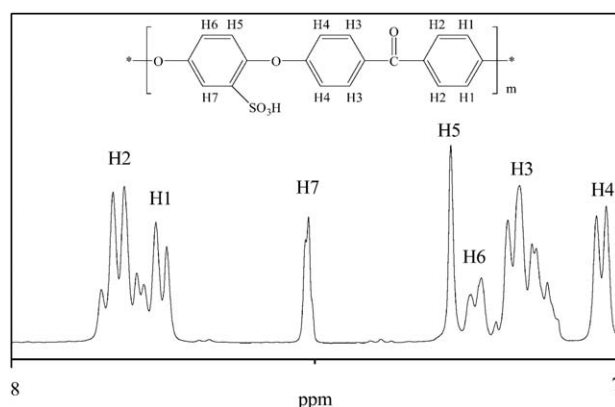

Figure 2. The ¹H-NMR spectra of SPEEK.

Table II. The Chemical Shifts of the Proton Designation of Each Position

Proton designation	H1	H2	H3	H4	H5	H6	H7
Chemical shift (ppm)	7.60	7.70~8.00	7.10~7.20	7.00	7.25	7.25	7.50
The peak area	0.6004	1	1.3407	0.6232	0.3801	0.3121	0.2848

As shown in Figure 3(d–f), the high loading of imidazole/$(HPO_3)_3$ will result in visible phase separation on the surface of SPEEK/imidazole/$(HPO_3)_3-3$, SPEEK/imidazole/$(HPO_3)_3-4$ and SPEEK/imidazole/$(HPO_3)_3-5$ composite membrane. The surface are covered with a layer of the gel of imidazole/$(HPO_3)_3$.

X-ray Diffraction

The typical XRD patterns of the pure SPEEK and SPEEK/imidazole/$(HPO_3)_3-3$ composite membrane are shown in Figure 6. XRD is used to identify the composite membrane crystalline structure. PEEK is a semicrystalline polymer, showing sharp crystalline peak in the 2θ range $20\sim30°$.[24,25] For the pure SPEEK and composite membrane [Figure 6(a)], a typical amorphous reflection peak ranging from 15 to 30° is observed. The amorphous structure of polymer SPEEK indicates the high sulfonation degree of PEEK.[26] In Figure 6(b), imidazole shows no crystalline peak at $2\theta = 22°$, 26°, and 32°,[27] which indicates that imidazole is dispersed in polymer matrix in amorphous state. These results show that the pure SPEEK membrane and the composite membranes are typical amorphous polymer. The amorphous structure of polymer electrolyte is beneficial to proton conductivity.

Thermal Analysis of the Composite Membranes

The TG results and DSC thermograms of the pure SPEEK and SPEEK/imidazole/$(HPO_3)_3-3$ composite membrane are illustrated in Figure 7. As can be seen in Figure 7, for the pure SPEEK membrane (prepared with DMSO), the TG curve exhibited a magnification of the three mass loss curves in the temperature of 25–300°C. At low temperature, two mass losses can be observed for pure SPEEK corresponding to about 12% of its initial mass. The first loss (below 100°C), accompanied by an endothermic peaks occurred at about 80°C, can be attributed to water molecules absorbed by hydrophilic groups and lost until the dry state of the sample is reached.[28–30] The second weight loss stage can be attributed to the loss of residual solvent DMSO.[30] The last distinct loss starts at ~210°C, with a continuous endothermic peak around 210–230°C, which is attributed to the decomposition of the sulfonic acid groups of SPEEK. From Figure 7(c), one can see that the glass transition temperature for pure SPEEK membrane is around 205°C.[7,31–33]

As can be seen in Figure 7, for the SPEEK/imidazole/$(HPO_3)_3-3$ composite membrane, the TG curve exhibited a continuous weight loss from 50 to 400°C, consisting of three weight loss stages. The first loss stage, which is at the
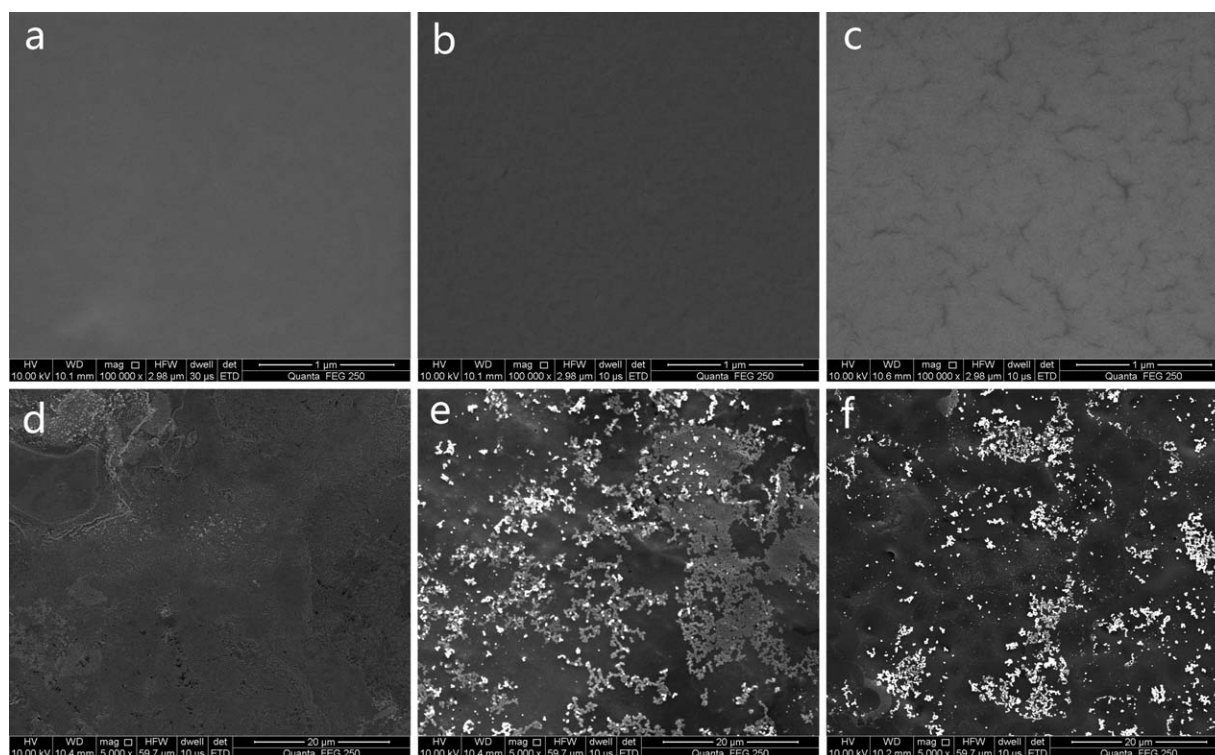

Figure 3. Typical SEM micrographs of pure SPEEK and SPEEK/imidazole/$(HPO_3)_3$ composite membranes: (a) SPEEK; (b) SPEEK/imidazole/$(HPO_3)_3-1$; (c) SPEEK/imidazole/$(HPO_3)_3-2$; (d) SPEEK/imidazole/$(HPO_3)_3-3$; (e) SPEEK/imidazole/$(HPO_3)_3-4$; (f)SPEEK/imidazole/$(HPO_3)_3-5$.
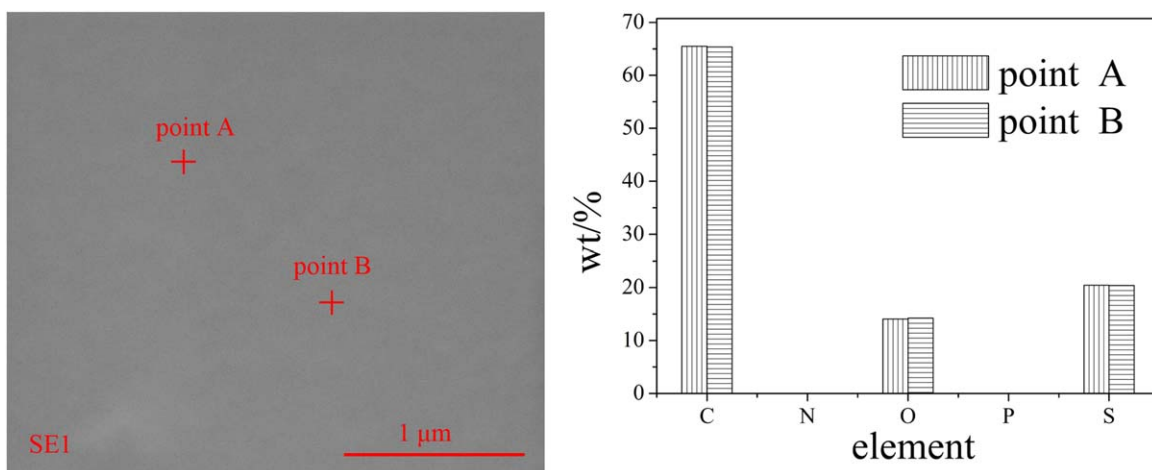
Figure 4. Element contents of pure SPEEK membrane by EDX. [Color figure can be viewed in the online issue, which is available at wileyonlinelibrary. com.]

temperature range from 60 to 150°C, is due to the volatilization of the absorbed humidity, as evidenced by a sharp endothermic peak at about 80°C. The second weight loss stage at 150–210°C can be attributed to the loss of residual solvent DMSO and the dehydration condensation reaction of phosphoric acid. There is the last distinct at 210–400°C. It could be due to the decomposition of the sulfonic acid groups of SPEEK and imidazole.

Proton Conductivity of the Composite Membranes

The proton conductivity of composite membrane at 55–135°C is shown in Figure 8. It can be seen from the figure that the proton conductivity of composite membranes increased with the content of imidazole/$(HPO_3)_3$ increasing, although the reduction occurred at the PEEK/imidazole/$(HPO_3)_3-5$ composite membrane. Furthermore, the proton conductivities of SPEEK/imidazole/$(HPO_3)_3-1$ and SPEEK/imidazole/$(HPO_3)_3-2$ composite membranes are lower than that of pure SPEEK membrane. For those composite membranes, the highest conductivity is about 3.8×10^{-3} S/cm for the SPEEK/imidazole/

$(HPO_3)_3-4$ composite membrane at 135°C, which is about one order higher than those at lower temperature of 55°C.

Kreuer K.D. reported that protons might transfer through hydrogen-bonded ionic channels such as imidazole under Imi-$ImiH^+$...Imi route.[7,34] For SPEEK/imidazole/$(HPO_3)_3$ composite membranes, imidazole/$(HPO_3)_3$ as proton reservoirs constructs numerous new proton-transfer pathways within the membranes and thus increases the membrane's proton conductivity. $(HPO_3)_3$ not only provides additional active sites for fast proton transfer, but also could be bound with sulfonic acid and imidazole groups through hydrogen bond.

Taking into account the results of Figure 3, the microstructure of pure SPEEK membrane and composite membranes is illustrated in Figure 9. As shown in Figure 9(a), the microstructure of pure SPEEK membrane and the proton-transfer pathway is relatively ordered.[35–37] However, for the composite membrane, with the doping of the hydrophilic group [e.g., imidazole, $(HPO_3)_3$], the relatively ordered structure of SPEEK polymer will be destroyed by the strong interaction between imidazole,
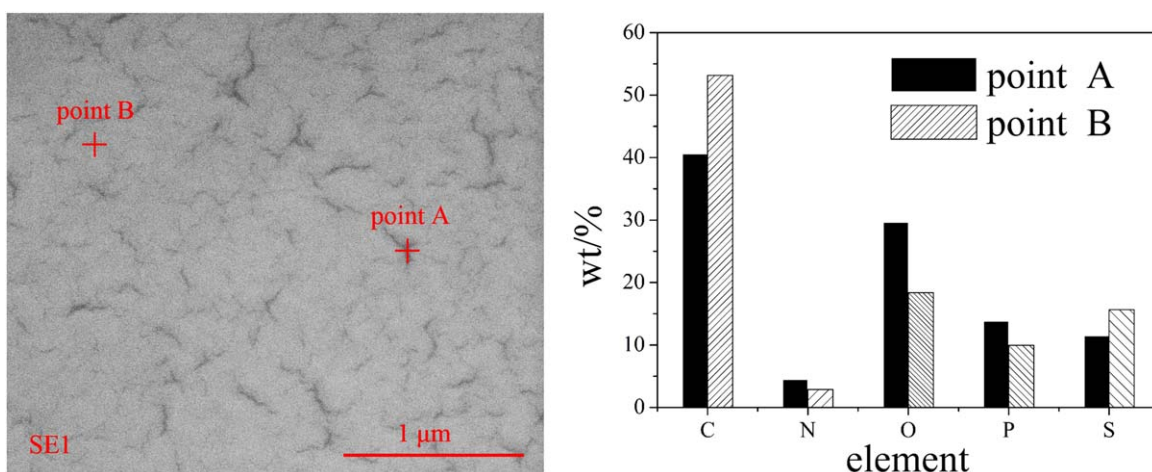

Figure 5. Element contents of SPEEK/imidazole/$(HPO_3)_3-2$ composite membrane by EDX. [Color figure can be viewed in the online issue, which is available at wileyonlinelibrary.com.]
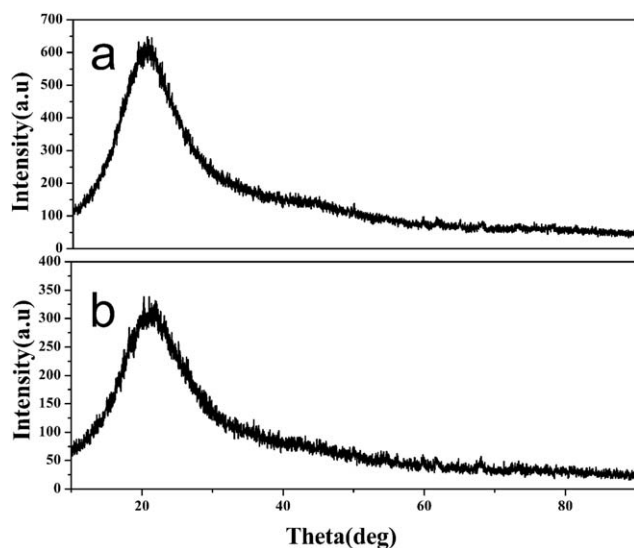
Figure 6. XRD pattern of pure SPEEK (a) and SPEEK/imidazole/$(HPO_3)_3-3$ composite membrane (b).

$(HPO_3)_3$ and $-SO_3H$, and some agglomeration of SPEEK/imidazole/$(HPO_3)_3$ will be formed as Figure 9(b) showed which influences the proton-transfer pathway. With the higher doping level [Figure 9(c)], the 3D space of the SPEEK polymer matrix is filled with imidazole/$(HPO_3)_3$ forming a new interconnecting proton conducting channels (phase sepration). The microstructure (Figure 9) is verified by the SEM images (Figure 3) and EDX spectra (Figures 4 and 5) of pure SPEEK membrane and composite membranes.

For a composite polymer membrane, the proton conductivity mainly results from the structure of polymer matrix and the concentration of proton carriers.[38] The conducting channels tend to be interconnected at higher imidazole/$(HPO_3)_3$ contents, while the conducting regions composed of imidazole/$(HPO_3)_3$ are isolated at lower imidazole/$(HPO_3)_3$ contents. Sulfonic acid in SPEEK can form hydrogen bonds with imidazole/
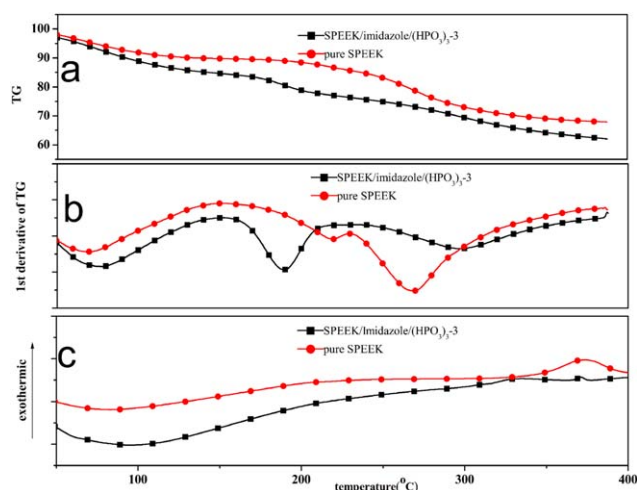

Figure 7. TG (a), DTG (b) and DSC (c) curves for pure SPEEK and SPEEK/imidazole/$(HPO_3)_3-3$ composite membrane. [Color figure can be viewed in the online issue, which is available at wileyonlinelibrary.com.]
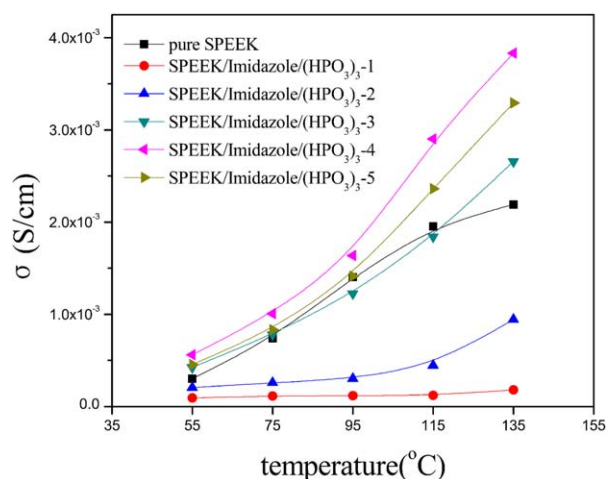

Figure 8. Proton conductivity of pure SPEEK and SPEEK/imidazole/$(HPO_3)_3$ composite membranes. [Color figure can be viewed in the online issue, which is available at wileyonlinelibrary.com.]

$(HPO_3)_3$ and constructed numerous proton-transfer pathways. An interconnected channel among SPEEK, imidazole and $(HPO_3)_3$ is formed at a high imidazole/$(HPO_3)_3$ contents. Furthermore, in Figure 3(d–f), with the higher doping level [Figure 9(c)], the 3D space of the SPEEK polymer matrix is filled with imidazole/$(HPO_3)_3$ and the surface of the membrane is also covered with imidazole/$(HPO_3)_3$. Noticed that the proton conductivity of the gel of imidazole/$(HPO_3)_3$ is much higher than that of pure SPEEK as shown in Supporting Information Figure S1, therefore, for the composite membrane, with lower doping content(≤ 28.6 wt %), the conductivity decreases mainly due to the polymer matrix structure destruction. With the doping content increase, the conductivity increases due to the formation of new proton conducting channel [the separated phase of imidazole/$(HPO_3)_3$]. This phenomenon is also observed in SPEEK/$(HPO_3)_3$ and SPEEK/imidazole composite membrane system, i.e., the proton conductivity of SPEEK/$(HPO_3)_3$ and SPEEK/imidazole composite membranes are both lower than that of pure SPEEK membrane. Proton conductivity of pure SPEEK, SPEEK/$(HPO_3)_3$ and SPEEK/imidazole composite membranes at $55\sim135°C$ is shown in Supporting Information Section S2.

As to the slight reduction of proton conductivity occurred at the SPEEK/imidazole/$(HPO_3)_3-5$ composite membrane. We cannot reasonably interpret this phenomenon at present, perhaps it is related with slight recrystallization of proton carriers, e.g., imidazole. Here, further study is still needed to clarify this phenomenon.

Mechanical Property

Good mechanical strength is essential for fuel cell application. The pure SPEEK and SPEEK/imidazole/$(HPO_3)_3-3$ composite membrane were tested for the tensile strengths of the membranes, as shown in Figure 10. All tested samples are ductile. These results suggest that the pure SPEEK membrane and composite membrane have maintained the highly mechanical property of 29.66 MPa and 20.21 MPa at 20°C, respectively. The slight reduction may be attributed to the crazing as evidenced by the SEM micrographs of SPEEK/imidazole/$(HPO_3)_3$
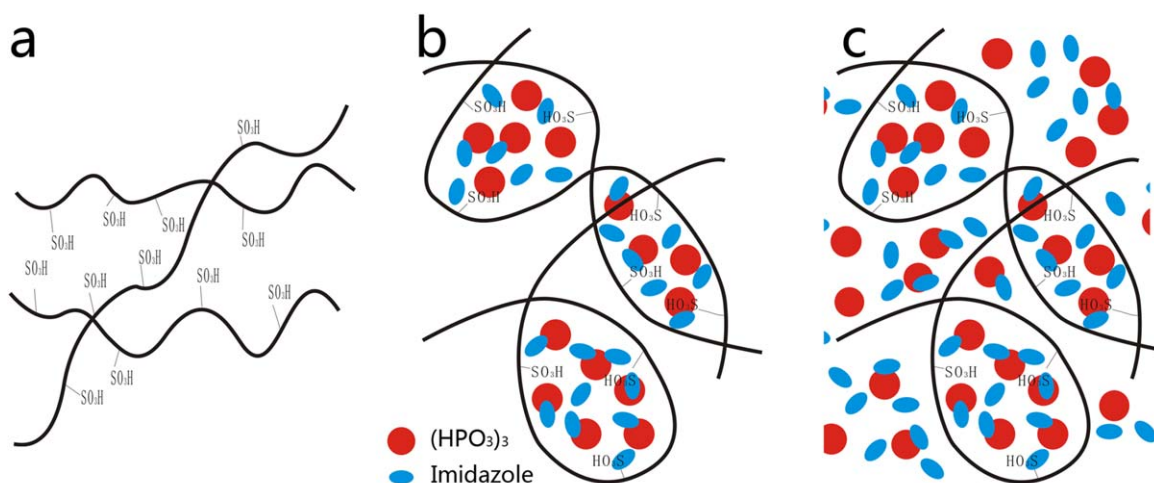
Figure 9. The microstructure of pure SPEEK membrane and composite membranes: (a) pure SPEEK membrane, (b) Composite membrane with lower doping level [e.g., SPEEK/imidazole/$(HPO_3)_3$−2 membrane], (c) Composite membrane with higher doping level (e.g. SPEEK/imidazole/$(HPO_3)_3$−4 membrane). [Color figure can be viewed in the online issue, which is available at wileyonlinelibrary.com.]

composite membranes [Figure 3(d)]. The tensile strength of the composite membrane is lower than that of SPEEK, probably due to an increase in imidazole/$(HPO_3)_3$ content. But the strength is almost equivalent to the value of Nafion® membrane which has been reported to be 15.5 MPa.[24,39]

CONCLUSIONS

A novel proton membrane based on SPEEK/imidazole/$(HPO_3)_3$ has been successfully prepared and characterized. The composite membranes were amorphous polymer and its thermal stability is slightly lower than that of pure SPEEK membrane. The strength of the SPEEK/imidazole/$(HPO_3)_3$ composite membranes is almost equivalent to the value of Nafion® membrane. Proton conductivity of SPEEK/imidazole/$(HPO_3)_3$ composite membranes increased with temperature. The composite membrane showed an increasing proton conductivity with the incorporation of imidazole/$(HPO_3)_3$ into SPEEK until 44.4wt % and decreased suddenly after further imidazole/$(HPO_3)_3$ addition. SPEEK/imidazole/$(HPO_3)_3$−4 composite membrane has an anhydrous proton conductivity as high as 3.8×10^{-3} S/cm at 135°C.

Figure 10. Stress strain curve of pure SPEEK and SPEEK/imidazole/$(HPO_3)_3$−3 composite membrane. [Color figure can be viewed in the online issue, which is available at wileyonlinelibrary.com.]

REFERENCES

1. Li, H.; Jiang, F.; Di, Z.; Gu, J. *Electrochim. Acta* **2012**, *59*, 86.

2. Silva, B. B.; Soares, J. B.; Malfatti, C. F.; Forte, M. *J. Membr. Sci.* **2011**, *374*, 12.

3. Nunes, S.; Ruffmann, B.; Rikowski, E.; Vetter, S.; Richau, K. *J. Membr. Sci.* **2002**, *203*, 215.

4. Silva, V.; Ruffmann, B.; Vetter, S.; Mendes, A.; Madeira, L.; Nunes, S. *Catal. Today* **2005**, *104*, 205.

5. Shibuya, N.; Porter, R. S. *Macromolecules* **1992**, *25*, 6495.

6. Lakshmi, R. M.; Choudhary, V.; Varma, I. *J. Mater. Sci.* **2005**, *40*, 629.

7. Jithunsa, M.; Tashiro, K.; Nunes, S. P.; Chirachanchai, S. *Int. J. Hydrogen Energy* **2011**, *36*, 10384.

8. Bozkurt, A.; Meyer, W. *Solid State Ionics* **2001**, *138*, 259.

9. Pu, H.; Meyer, W. H.; Wegner, G. *J. Polym. Sci. Part B: Polym. Phys.* **2002**, *40*, 663.

10. Martinez, M.; Molmeret, Y.; Cointeaux, L.; Iojoiu, C.; Leprêtre, J.-C.; El Kissi, N.; Judeinstein, P.; Sanchez, J.-Y. *J. Power Sources* **2010**, *195*, 5829.

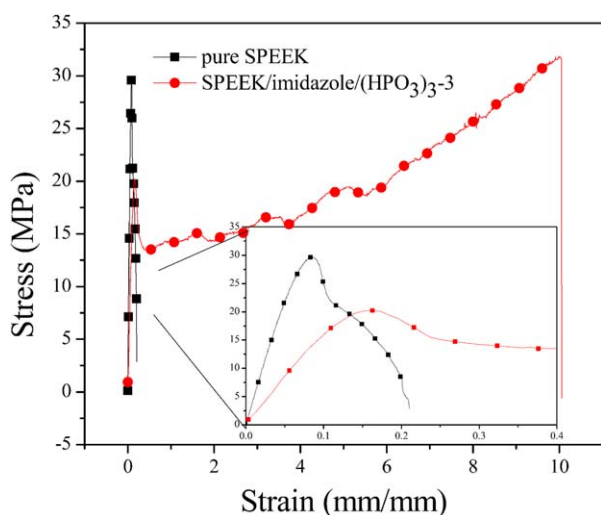11. Deligöz, H.; Yılmazoğlu, M. *J. Power Sources* **2011**, *196*, 3496.

12. Qin, Q.; Tang, Q.; Li, Q.; He, B.; Chen, H.; Wang, X.; Yang, P. *Int. J. Hydrogen Energy* **2014**, *39*, 4447.

13. Speight, J. G. Lange's Handbook of Chemistry; McGraw-Hill: New York, **2005**.

14. Smitha, B.; Sridhar, S.; Khan, A. *J. Membr. Sci.* **2005**, *259*, 10.

15. Jarumaneeroj, C.; Tashiro, K.; Chirachanchai, S. *J. Power Sources* **2014**, *249*, 185.

16. Kawada, A.; McGhie, A.; Labes, M. *J. Chem. Phys.* **2003**, *52*, 3121.

17. Şengül, E.; Erdener, H.; Akay, R. G.; Yücel, H.; Baç, N.; Eroğlu, İ. *Int. J. Hydrogen Energy* **2009**, *34*, 4645.

18. Mikhailenko, S.; Zaidi, S.; Kaliaguine, S. *Catal. Today* **2001**, *67*, 225.

19. Pu, H.; Wang, D. *Electrochim. Acta* **2006**, *51*, 5612.

20. Yamada, M.; Honma, I. *Angew. Chem. Int. Ed.* **2004**, *43*, 3688.

21. Wu, H.; Shen, X.; Cao, Y.; Li, Z.; Jiang, Z. *J. Membr. Sci.* **2014**, *451*, 74.

22. Boroglu, M. S.; Celik, S. U.; Bozkurt, A.; Boz, I. *J. Membr. Sci.* **2011**, *375*, 157.

23. Zaidi, S. J.; Mikhailenko, S.; Robertson, G.; Guiver, M.; Kaliaguine, S. *J. Membr. Sci.* **2000**, *173*, 17.

24. Li, H.; Chen, X.; Jiang, F.; Ai, M.; Di, Z.; Gu, J. *J. Power Sources* **2012**, *199*, 61.

25. Cao, J.; Su, W.; Wu, Z.; Kitayama, T.; Hatada, K. *Polymer* **1994**, *35*, 3549.

26. Krishnan, P.; Park, J.-S.; Kim, C.-S. *J. Membr. Sci.* **2006**, *279*, 220.

27. Pu, H.; Luo, M.; Yang, Z. *Eur. Polym. J.* **2007**, *43*, 5076.

28. Carbone, A.; Pedicini, R.; Portale, G.; Longo, A.; D'Ilario, L.; Passalacqua, E. *J. Power Sources* **2006**, *163*, 18.

29. Marani, D.; Di Vona, M.; Traversa, E.; Licoccia, S.; Beurroies, I.; Llewellyn, P.; Knauth, P. *J. Phys. Chem. B* **2006**, *110*, 15817.

30. Di Vona, M.; Sgreccia, E.; Donnadio, A.; Casciola, M.; Chailan, J.; Auer, G.; Knauth, P. *J. Membr. Sci.* **2011**, *369*, 536.

31. Schmittinger, W.; Vahidi, A. *J. Power Sources* **2008**, *180*, 1.

32. Krishnan, P.; Park, J.-S.; Yang, T.-H.; Lee, W.-Y.; Kim, C.-S. *J. Power Sources* **2006**, *163*, 2.

33. Krishnan, P.; Park, J.-S.; Kim, C.-S. *Eur. Polym. J.* **2007**, *43*, 4019.

34. Kreuer, K.-D.; Paddison, S. J.; Spohr, E.; Schuster, M. *Chem. Rev.* **2004**, *104*, 4637.

35. Li, M.; Zhang, G.; Xu, S.; Zhao, C.; Han, M.; Zhang, L.; Jiang, H.; Liu, Z.; Na, H. *J. Power Sources* **2014**, *255*, 101.

36. Jeon, J.-H.; Kang, S.-P.; Lee, S.; Oh, I.-K. *Sensor. Actuat. B-Chem.* **2009**, *143*, 357.

37. Zhang, N.; Zhang, G.; Xu, D.; Zhao, C.; Ma, W.; Li, H.; Zhang, Y.; Xu, S.; Jiang, H.; Sun, H.; Na, H. *Int. J. Hydrogen Energy* **2011**, *36*, 11025.

38. Tang, Q.; Qian, G.; Huang, K. *RSC Adv.* **2012**, *2*, 10238.

39. Kang, D. H.; Kim, D. *Korean J. Chem. Eng.* **2007**, *24*, 1101.